Nuclear Medicine and Biology 40 (2013) 280–288

Contents lists available at SciVerse ScienceDirect

Nuclear Medicine and Biology

journal homepage: www.elsevier.com/locate/nucmedbio

Radiolabelling and preliminary evaluation of ^{68}Ga-tetrapyrrole derivatives as potential tracers for PET

Frederic Zoller [a,b], Patrick J. Riss [a,c], Franz-Peter Montforts [d], Debra K. Kelleher [e], Elisabeth Eppard [a], Frank Rösch [a,*]

[a] Institute of Nuclear Chemistry, University of Mainz, Fritz-Strassmann-Weg 2, 55128, Mainz, Germany
[b] DKFZ, Clinical Cooperation Unit Nuclear Medicine, Im Neuenheimer Feld 280, 69120 Heidelberg, Germany
[c] The Wolfson Brain Imaging Centre, University of Cambridge, Box 65 Addenbrooke's Hospital,CB2 0QQ Cambridge, UK
[d] Institute of Organic Chemistry, University of Bremen, Leobener Straße NW 2C, 28359 Bremen, Germany
[e] Institute of Functional and Clinical Anatomy, University Medical Centre of the Johannes Gutenberg, University Mainz, Johann-Joachim-Becher-Weg 13, 55128 Mainz, Germany

ARTICLE INFO

Article history:
Received 17 October 2011
Received in revised form 10 November 2012
Accepted 15 November 2012

Keywords:
Gallium-68
Metalloporphyrin
Microwave-enhanced radiosynthesis
PET
Cancer

ABSTRACT

Tetrapyrroles are multisided natural products which are of relevance in clinical medicine. Owing to their specific accumulation in tumour tissue, porphyrins, metalloporphyrins and chlorins have been used as in photodynamic therapy and optical imaging. Moreover, their specific uptake into inflammatory atheromatous plaques via LDL endocytosis has been reported. The present study is concerned with the synthesis of ^{68}Ga labelled porphyrin derivatives and an in vitro assessment of the utility of radiotracers in positron emission tomography. A set of five porphyrin derivatives were labelled using ^{68}Ga from a commercially obtained radionuclide generator. Dedicated post-processing of the generator eluate was conducted to allow for labelling in aqueous media and also under anhydrous conditions. Challenge studies and incubation in human serum confirmed the stability of the tracers. Plasma protein binding was investigated in order to confirm the presence of freely diffusible radioligand in plasma. A preliminary microPET study in a tumour-bearing rat resulted in a clear visualisation of the tumour.

1. Introduction

$^{68}Ga^{III}$ is a pretentious radionuclide for clinical PET imaging. In terms of decay properties, it provides high positron abundance (89%) together with irrelevant photon emission (1.077 keV, 3.22%) and a half-life (68 min) compatible with the pharmacokinetic profile of most small molecule imaging agents. Being readily available from inexpensive ^{68}Ge/^{68}Ga-radionuclide generator systems [1–3] paired with straightforward labelling chemistry renders gallium-68 well suited for PET imaging in peripheral tissues.

In essence, most applications of the radionuclide are based on complexation of $^{68}Ga^{III}$ to a tetracoordinate to hexacoordinate chelator which itself is conjugated to a bioactive targeting moiety [4]. In the present study, however, our effort was guided by the inherent similarity of Ga^{III} and Fe^{III} complexes of planar tetrapyrroles, i.e. porphyrins and chlorins (Scheme 1).

Tetragonal pyramidal Fe^{III}-porphyrin complexes are abundant in nature and Fe^{II}/Fe^{III} redox-reactions in polypyrroles play a crucial role in biological systems. The above mentioned similarity can be attributed to similarities in size (van der Waals radius Ga^{3+} = 62 pm, Fe^{3+} = 65 pm) and electron configuration (Ga^{3+}: [Ar]3d^{10}; Fe^{3+}: [Ar]3d^{5}) [5,6]. Consequently, non-radioactive Ga-porphyrin complexes have been described in literature [7].

Porphyrin and chlorin derivatives selectively accumulate in tumour lesions and in inflammatory tissue [8]. Interaction with plasma proteins such as low density lipoprotein (LDL), transferrin and human serum albumin (HSA) are believed to be the key mechanisms for tumour uptake [9,10]. In this context, the use of porphyrin derivatives is already established both in the field of photodynamic therapy (PDT) and optical imaging [8,11]. Moreover, tetrapyrrole derivatives have been considered as targeting vectors for endoradiotherapy [12,13], boron neutron capture therapy [14], drug delivery [15] or sonodynamically induced apoptosis [16]. Imaging studies using spectrofluorometry or radiolabelled porphyrins have also been described [17–20]. In these cases, $^{64}Cu^{II}$ ($t_{1/2}$ = 12.7 h), $^{99m}Tc^{II}$ ($t_{1/2}$ = 6 h) and $^{65}Zn^{II}$ ($t_{1/2}$ = 244.26 d) were used as radionuclides. Among these radionuclides, only ^{99m}Tc is an appropriate radionuclide for routine clinical application, ^{64}Cu and ^{65}Zn are of minor interest due to their adverse radionuclide properties [21].

Based on the hypothesis that ^{68}Ga-labelled tetrapyrroles might provide a new option for PET imaging in oncology, we have devised a methodology for radiolabeling and purification of such complexes. The *in vitro* stability and plasma protein binding of the novel

* Corresponding author. Tel.: +49 6131 392 5302; fax: +49 6131 392 4692.
E-mail address: frank.roesch@uni-mainz.de (F. Rösch).

0969-8051/$ – see front matter © 2013 Elsevier Inc. All rights reserved.
http://dx.doi.org/10.1016/j.nucmedbio.2012.11.006

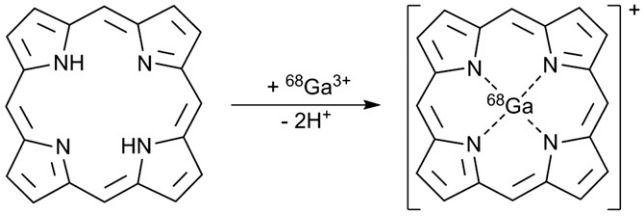

Scheme 1. General scheme of the [^{68}Ga]Ga^{III} coordination of the tetrapyrrole system.

compounds were investigated. A preliminary micro-PET study was conducted in a rat tumour model to proof the potential of ^{68}Ga-labelled tetrapyrroles as molecular imaging probe.

2. Materials and methods

2.1. General

All chemicals were obtained from Sigma-Aldrich (Sigma-Aldrich, Schnelldorf, Germany) and used without further purification. Hematoporphyrin (**1**; 8,13-bis(1-hydroxyethyl)-3,7,12,17-tetramethyl-21*H*,23*H*-porphine-2,18-dipropionic acid), protoporphyrin IX (**2**; 3,7,12,17-tetramethyl-8,13-divinyl-2,18-porphinedipropionic acid) and meso-tetraphenylporphyrin (**3**) were purchased in the highest available purity. The chlorins (3-(1-hydroxyheptyl)deuteron-porphyrin dimethylester (**4**) and ([(2R)-2-methoxycarbonylmethyl)-3-oxo-2,7,12,18-tetramethyl-2,3-dihydro-21H,23H-dihydroporphyrinato-13,17-diyl]dipropionic acid dimethylester) (**5**) were synthesised as described previously [22,23]. The cation exchange resin AG 50W-X8 (<400 mesh) was obtained from Bio-Rad. Sep-Pak® Accell plus light QMA cartridges were purchased from Waters (Waters GmbH, Eschborn, Germany). Milli-Q water (18.2 MΩcm^{-1}; Millipore GmbH, Schwalbach, Germany) was used in all aqueous procedures. Dulbecco's phosphate-buffered saline (DPBS) was obtained from Invitrogen (Life Technologies GmbH, Darmstadt, Germany). ^{68}Ge/^{68}Ga-radionuclide generators (50 mCi, 1.685 GBq) were obtained from Cyclotron Co. Ltd. (Obninsk, Russian Federation). Typically, batch activities of 50 to 300 MBq ^{68}Ga were used. Counting was performed in a well counter (Nuklear-Medizintechnik Dresden GmbH, Germany). Radiosyntheses under microwave irradiation were conducted in a CEM Discover® focused microwave synthesis system (CEM, Kamp-Lintfort, Germany) using dedicated 10 ml-reaction vessels. Radio thin layer chromatography (radio-TLC) was performed on reversed phase (RP-18 F_{254}, 5×7.5 cm, Merck) or silica gel (silica gel 60 F_{254}, 5×7.5 cm, Merck) coated aluminium TLC-sheets and analyzed using a flatbed imaging scanner (Instant Imager, Canberra Packard, Schwadorf, Austria). Radio-HPLC was performed using a solvent delivery system (S1121, Sykam GmbH, Eresing, Germany) connected to a UV/VIS-detector (UVIS 200, Linear, λ = 405 nm) and a radioactivity detector at 511 keV (ISOMED 110, Nuklear-Medizintechnik Dresden GmbH). An analytical RP-HPLC column (LiChroSorb®, RP-18, 7 µm, 250×4.6 mm, Merck) was used for quality control. Size-exclusion chromatography (SE-HPLC) was performed on a Waters HPLC-system (binary HPLC Pump 1525) connected to a UV/VIS detector (Dual Absorbance Detector 2487, Waters; λ = 280 nm) and a radioactivity detector (Radioflow Detector LB 509, EG&G Berthold, Bad Wildbad, Germany). An SE-HPLC column (Phenomenex HiTrap™ Desalting, 5 ml) was used as stationary phase.

2.2. ^{68}Ge/^{68}Ga generator and post-processing

A ^{68}Ge/^{68}Ga generator post-processing setup was applied as published previously [24,25]. [^{68}Ga]Ga^{III} was eluted using 0.1 M HCl (10 ml). The eluate was passed through a column containing AG 50 W-X8 resin (SCX; 50 mg loose packing, 3 mm column diameter), in order to remove trace impurities of Fe^{III}, ^{68}Zn^{III}, Ti^{IV} and ^{68}Ge^{IV}, the resin was rinsed with a mixture of acetone and 0.15N HCl (8:2, 1 ml) and provisionally dried.

For labelling in aqueous media, the ^{68}Ga trapped on the SCX column was eluted with a solution of 0.05 M HCl in acetone (2.4%, 400 µl). To optimize the desorption of [^{68}Ga]Ga^{III}, the SCX column was charged with the solution (150 µl) and allowed to equilibrate with the resin-bound ^{68}Ga for 2 min, followed by subsequent application of the remaining 250 µl.

For labelling under anhydrous conditions [25], the SCX column was thoroughly dried by a gentle stream of argon for 1 min to remove the residual solvent. Subsequently, the purified ^{68}Ga was eluted from the SCX column using a solution of 2% acetylacetone (acac) in acetone (600 µl).

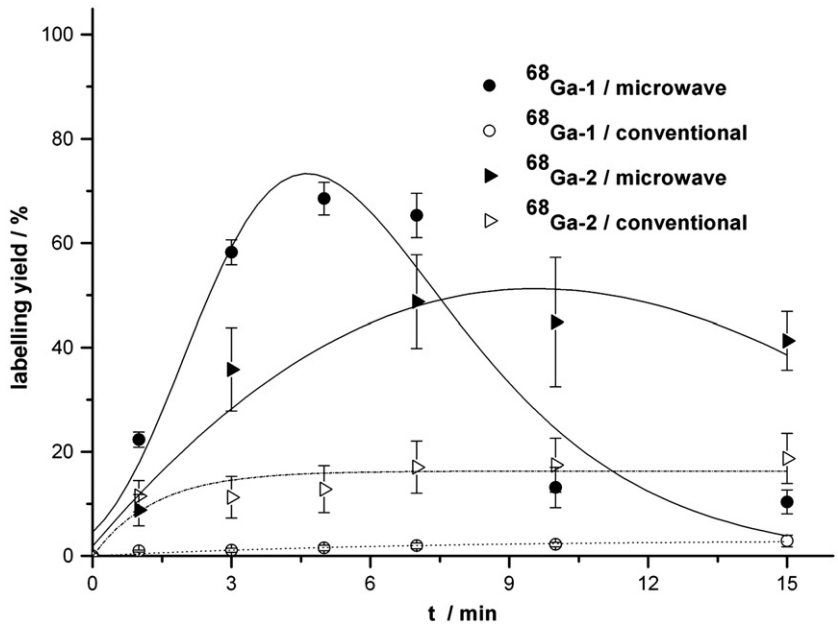

Fig. 1. Comparison of the time dependency of the labelling yield of [^{68}Ga]-**1** and [^{68}Ga]-**2** in HCl-acetone aqueous solution under conventional conditions (oil bath at 90 °C) and under microwave irradiation (170 °C, max. 150 W). Mean and standard deviation (mean ± SD, n = 3) were determined.

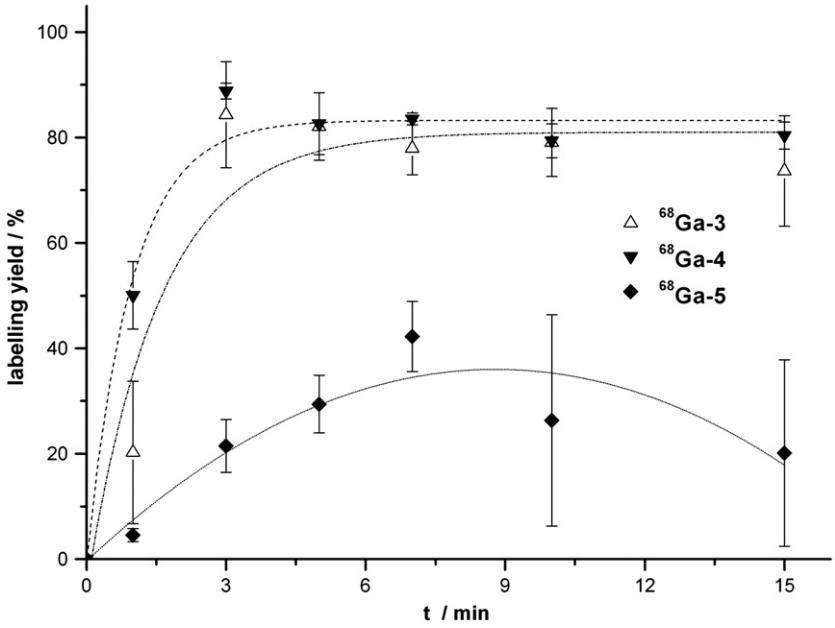

Fig. 2. Time dependency of the labelling yield of [^{68}Ga]-**3**, [^{68}Ga]-**4** and [^{68}Ga]-**5** in chloroform solution using a constant microwave irradiation (170 °C, 300 W). Mean and standard deviation (mean ± SD, n = 3) were determined.

In both cases, the SCX resin was reconditioned with 4 M HCl (1 ml) followed by water (1 ml).

2.3. Radiochemistry

2.3.1. Labelling in aqueous media

Labelling precursor **1** (20 μl, 33 nmol, 1 mg/ ml acetone) or **2** (20 μl, 36 nmol, 1 mg/ml acetone) was added to a glass vial containing H_2O (5 ml) and warmed to 70 °C in an oil bath. A solution of 0.05 M HCl in acetone (2.4%, 400 μl) containing the purified ^{68}Ga activity (50-300 MBq) was added. The mixture was heated to 90 °C for 15 min. In case of microwave-enhanced radiosynthesis, the respective mixtures were heated up to 170 °C in a sealed vessel using a microwave irradiation of up to 150 W for the same period of time. Samples were withdrawn from the reaction mixture after 1, 3, 5, 7, 10 and 15 minutes and labelling yields were determined by radio-TLC.

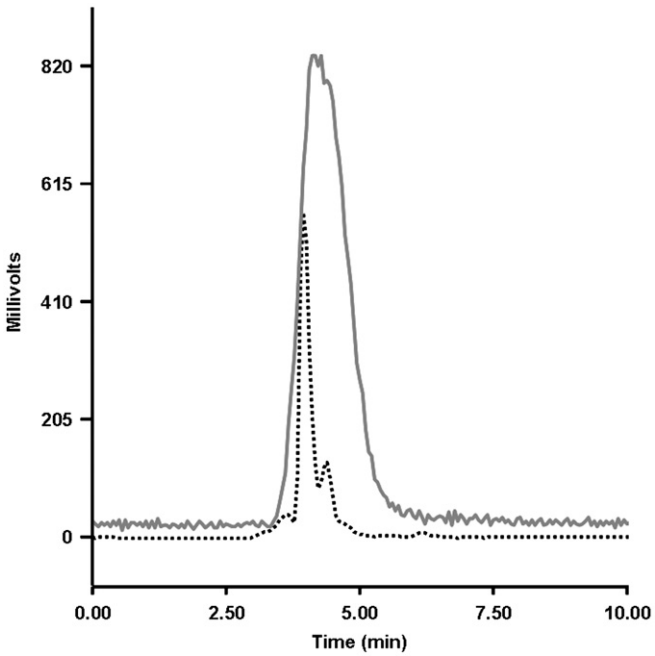

Fig. 3. Radio-HPLC chromatogram of ^{68}Ga-**1** showing radiochemical purity of the tracer after purification by solid-phase extraction. HPLC-conditions: MeCN: H_2O 95:5 (v/v) + 0.1% TFA; 0.5 ml/min. UV-Trace at 405 nm (dashed line) and radio trace (solid line).

2.3.2. Labelling under anhydrous conditions

Labelling under anhydrous conditions was conducted in $CHCl_3$ using [^{68}Ga](acac)$_3$ as labelling agent, which was generated as previously reported [25]. The $CHCl_3$ solution, containing about 85% of [^{68}Ga]Ga(acac)$_3$, was added to a suspension containing 5 mg (32 μmol) 2,5-dihydroxy benzoic acid (DHBA), 20 μL of the corresponding tetrapyrrole solution (**3**: 33 nmol, 1 mg/ml in $CHCl_3$; **4**: 34 nmol, 1 mg/ml in $CHCl_3$; **5**: 34 nmol, 1 mg/ml in $CHCl_3$) in 280 μL chloroform. The labelling mixtures were heated in a sealed vessel using a constant microwave irradiation of 300 W for 1 to 15 min. Labelling yields after a reaction time of 1, 3, 5, 7, 10 and 15 minutes were determined by radio-TLC.

2.3.3. Purification of the labelled compounds

Purification of the products was performed using an anion exchange cartridge (QMA Sep-Pak®; preconditioned with 5 ml 1 M K_2CO_3 and 5 ml H_2O, followed by 20 ml air). For purification of [^{68}Ga]-**1** and [^{68}Ga]-**2**, the reaction mixture was cooled to ambient temperature, passed through the QMA cartridge, and the cartridge was washed with H_2O (200 μl). The purified products were eluted with DPBS solution (500 μl), whereas non-chelated ^{68}Ga-activity was retained on the cartridge under these conditions.

Table 1
Summarized radiochemical results of porphyrin derivatives.

Compound	[^{68}Ga]-**1**	[^{68}Ga]-**2**	[^{68}Ga]-**3**	[^{68}Ga]-**4**	[^{68}Ga]-**5**
Labelling yield [%][a]	69 ± 3	49 ± 9	82 ± 6	83 ± 6	42 ± 7
RCY [%][b]	33 ± 4	22 ± 8	73 ± 6	50 ± 9	-/-
RCP [%][c]	95 ± 1	85 ± 10	98 ± 1	95 ± 2	-/-
Total time of synthesis [min]	14	14	16	16	-/-

Total time of synthesis compromises post-processing of the generator eluate, labelling and purification process (RCY: decay corrected overall radiochemistry yield; RCP: radiochemical purity; [a]TLC yields for the incorporation of ^{68}Ga into the molecules; [b]isolated and formulated yield after SPE; [c]purity of the formulation).

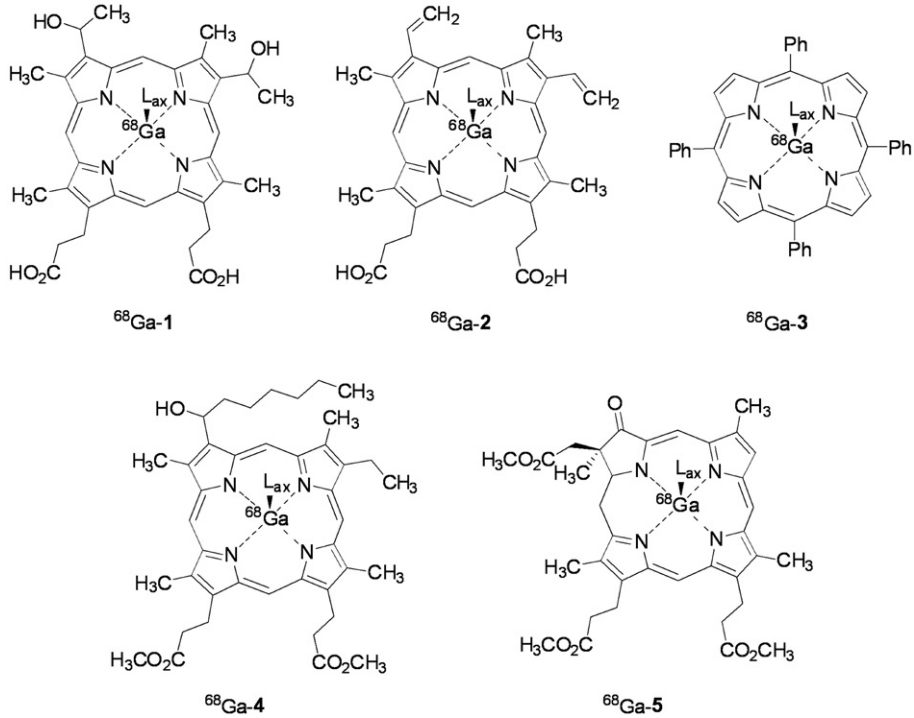

Fig. 4. Proposed structures of the ^{68}Ga-labelled porphyrins derivatives. The axial co-ligand (L_{ax}) is represented by chloride in [^{68}Ga]-**1** and [^{68}Ga]-**2**, whereas in [^{68}Ga]-**3**, [^{68}Ga]-**4** and [^{68}Ga]-**5** the axial co-ligand is substituted by 2,5-dihydroxy benzoic acid. (**1**: hematoporphyrin (8,13-bis(1-hydroxyethyl)-3,7,12,17-tetramethyl-21*H*,23*H*-porphine-2,18-dipropionic acid); **2**: proto-porphyrin IX (3,7,12,17-tetramethyl-8,13-divinyl-2,18-porphinedipropionic acid); **3**: *meso*-tetraphenylporphyrin (5,10,15,20-tetraphenylporphin); **4**: 3-(1-hydroxyheptyl)-*deutero*-porphyrin dimethylester; **5**: ([(2R)-2-methoxycarbonylmethyl)-3-oxo-2,7,12,18-tetramethyl-2,3-dihydro-21H,23H-dihydroporphyrinato-13,17-diyl]dipropionic acid dimethylester.

For purification of [^{68}Ga]-**3**-DHBA and [^{68}Ga]-**4**-DHBA, the reaction mixtures were cooled to 50 °C and the solvent was evaporated to dryness under a gentle stream of argon. The solid residue was re-dissolved in ethanol (400 μl) and passed through an anion exchange cartridge (QMA Sep-Pak®; preconditioned with 5 ml 1 M K_2CO_3, 5 ml H_2O, followed by 20 ml air). The resin-bound radioactivity was washed with water (3 ml) and eluted with DPBS solution (2 ml). In parallel, non-chelated amounts of ^{68}Ga-activitity were retained on the resin.

2.3.4. Quality control

Labelling yields and radiochemical purities (RCP) were determined by radio-TLC using both reverse phase and silica TLC sheets. Five different mobile phases were used (a: silica gel, 0.01 M HCl-EtOH, 3:1; b: silica gel, 0.01 M sodium citrate; c: silica gel, $CHCl_3$-MeOH, 9:1; d: silica gel, $CHCl_3$-MeOH, 7:2; e: RP-18, ethyl acetate-ethanol, 1:1). Corresponding R_f values were: [^{68}Ga]-**1**: R_f (a) = 0.9, R_f (b) = 0.0; [^{68}Ga]-**2**: R_f (a) = 0.9, R_f (b) = 0.0; [^{68}Ga]-**3**-DHBA: R_f (c) = 0.6, R_f (e) = 1.0; [^{68}Ga]-**4**-DHBA: R_f (d) = 0.5, R_f (e) = 1.0; [^{68}Ga]-**5**-DHBA: R_f (d) = 0.9, R_f (e) = 1.0; ^{68}Ga: R_f (a,e,d,e) = 0.0, R_f (b) = 1.0.

In addition, radio-HPLC was performed under isocratic conditions (MeCN: H_2O 95:5 (v/v) + 0.1% TFA; 0.5 ml/min). The compounds were eluted after the following retention times (t_R): [^{68}Ga]$GaCl_3$: t_R = 7.8 min, 1: t_R = 3.3 min, [^{68}Ga]-**1**: t_R = 4.5 min; **2**: t_R = 3.9 min; [^{68}Ga]-**2**: t_R = 4.4 min; **3**: t_R = 13.8 min; [^{68}Ga]-**3**-DHBA, t_R = 11.3 min; **4**: t_R = 28.5 min; [^{68}Ga]-**4**-DHBA, t_R = 13.5 min.

2.4. In vitro stability

2.4.1. Transchelation and transmetallation

Kinetic inertness and thermodynamic stability of the labelled products were confirmed by challenge studies in DTPA solution (1 μM and 1 mM), $FeCl_3$ solution (1 μM) and *apo*-transferrin solution (1 mg/ml in DPBS (1×)). Aliquots of 1-3 MBq of the purified products were added to the appropriate solutions (200 μl) and incubated under gentle agitation at 37 °C. The composition of the mixtures was monitored by analysing 1 μl aliquots with radio-TLC at selected time points for up to 2 hours.

2.4.2. Serum stability

Human serum was isolated from heparinised full blood by centrifugation at 5000 rpm for 5 min. 1-3 MBq of the respective purified product solution was added to human serum (200 μl) and incubated under gentle agitation at 37 °C. The composition of the samples was monitored by analysing 1 μl aliquots with radio-TLC at selected time intervals for up to 2 hours.

2.5. Plasma protein binding

For the determination of HSA binding, an aliquot of the respective purified ^{68}Ga-polypyrrole (100 ml, 1-3 MBq) was added to a HSA solution (1 ml, 1 mg/ml in DPBS (1×)) and incubated under gentle agitation at 37 °C for 2 hours. At selected time points, 100 μl samples

Table 2
Complex stability of the labelled tetrapyrrole derivatives in terms of transchelation (incubation in DTPA solutions, n = 3) and transmetalation reactions (incubation in $FeCl_3$ solution, n = 3).

Incubation solution	Labelled compound	Intact labelled compound/%					
		0 min	15 min	30 min	60 min	90 min	120 min
1 μM DTPA	[^{68}Ga]-**1**	100 ± 0	91 ± 9	93 ± 7	88 ± 0	95 ± 4	91 ± 5
	[^{68}Ga]-**3**	100 ± 0	99 ± 0	97 ± 1	98 ± 1	97 ± 1	93 ± 3
	[^{68}Ga]-**4**	100 ± 0	94 ± 6	95 ± 5	94 ± 6	93 ± 3	92 ± 4
1 mM DTPA	[^{68}Ga]-**1**	100 ± 0	94 ± 6	95 ± 5	87 ± 12	92 ± 8	96 ± 3
	[^{68}Ga]-**3**	100 ± 0	97 ± 1	99 ± 0	93 ± 3	97 ± 0	98 ± 1
	[^{68}Ga]-**4**	100 ± 0	87 ± 2	86 ± 7	84 ± 5	76 ± 6	77 ± 2
1 μM $FeCl_3$	[^{68}Ga]-**1**	100 ± 0	93 ± 1	92 ± 1	92 ± 1	92 ± 1	88 ± 0
	[^{68}Ga]-**3**	100 ± 0	98 ± 1	99 ± 0	96 ± 3	96 ± 1	98 ± 0
	[^{68}Ga]-**4**	100 ± 0	89 ± 5	95 ± 2	99 ± 4	96 ± 4	93 ± 7

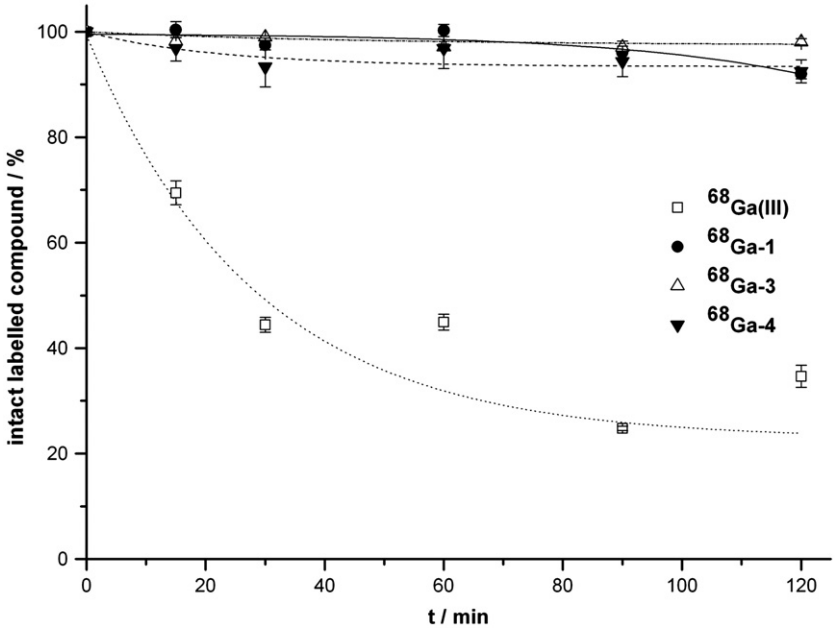

Fig. 5. Complex stability of the ^{68}Ga-labelled tetrapyrrole derivatives and behaviour of non-chelated ^{68}Ga in the presence of *apo*-transferrin (n = 3). The ability of *apo*-transferrin to chelate ^{68}Ga under these conditions has been validated by incubation with an aliquot of the generator eluate.

were withdrawn from the mixture and injected into an SE-HPLC, phosphate buffer (0.1 M, pH 7.2; 0.5 ml/min) was used as mobile phase. A sample of non-chelated gallium-68 was treated in the same way. For assessment of LDL uptake, the same procedure was followed as described for HSA binding, using 1 ml of an LDL solution (0.5 mg/ml in DPBS (1×)).

The porphyrin protein aggregates formed were detected as follows: HSA porphyrin complex: $t_R = 3.8$ min; LDL-porphyrin-complex: $t_R = 3.7$ min. The unbound tracers eluted after the following retention times (t_R): $^{68}Ga^{III}$: $t_R = 8.2$ min, ^{68}Ga-**1**: $t_R = 8.0$ min; [^{68}Ga]-**3**-DHBA, $t_R = 8.4$ min; [^{68}Ga]-**4**-DHBA, $t_R = 8.2$ min. The aggregation of each compound to the proteins was evaluated by integration of the relevant radioactivity peak of the corresponding chromatogram.

2.6. MicroPET imaging

Solid tumours grew subcutaneously following injection of a suspension of DS sarcoma cells into the hind foot dorsum of the left and right leg of a male Sprague-Dawley rat (Charles River Wiga, Sulzfeld, Germany) with a body weight of approximately 200 g. Tumours grew for seven days prior to PET imaging. On the day of the PET scan the animal was anaesthetized with an intra peritoneal injection of sodium pentobarbital (40 mg/kg, Narcoren®, Merial, Germany), with further doses of anaesthetic being given as necessary during the imaging procedures. A catheter was then placed in the left carotid artery for tracer administration. The animal was placed on the bed of a Siemens/CTI Focus 150 small animal PET scanner. The animal received an infusion

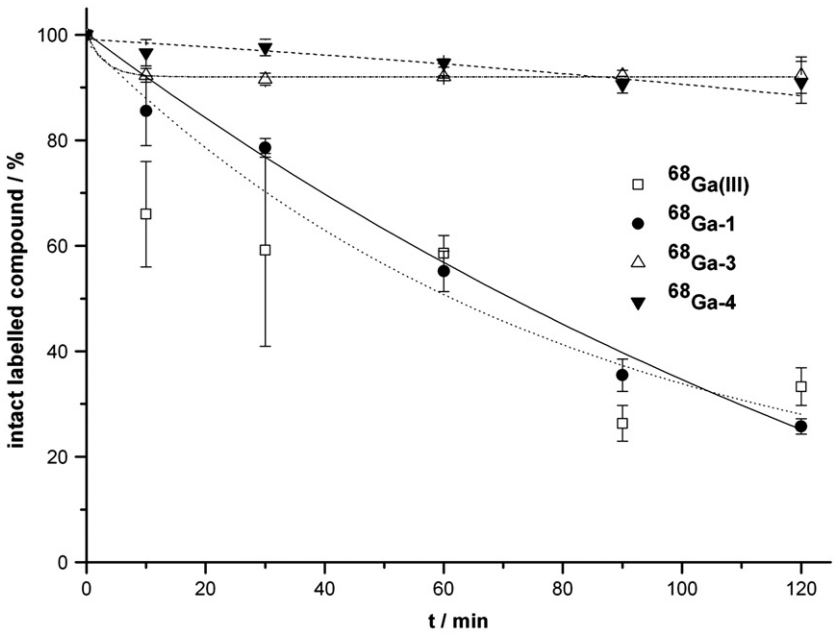

Fig. 6. Stability of ^{68}Ga-labelled porphyrin derivatives and non-chelated gallium-68 in human serum incubated at 37 °C. Mean and standard deviation (mean ± SD, n = 3) were determined.

of 19 MBq [^{68}Ga]-**1** in 0.9 mL PBS via the arterial catheter and dynamic PET data was acquired for 60 min. Afterwards, a 20-min whole body scan was performed from the same animal placed. The reconstructed PET data was analysed using pmod software. List-mode data acquisition was used for PET image and reconstruction of time-activity-curves. Three-dimensional regions of interest (ROI) were drawn onto the PET data and the radioactivity concentration per volume (%ID/ml) of tumour tissue was computed. The testes were chosen as regions of reference. Whole body PET image were generated 60-80 min p.i. performing data reconstruction using OSEM-mode algorithm.

2.7. Ex vivo biodistribution

Radioactivity amounts of 10 to 20 MBq of [^{68}Ga]-**1** in PBS were injected via the tail vein of female 4- to 6-week old XY rats (Charles River WIGA, Sulzfeld, Germany). At defined time points post injection, the n (n = 3) were sacrificed, and selected tissue samples (heart, lung, spleen, liver, kidney, muscle, intestine, brain and duodenum) were removed, drained of blood, weighed, and the radioactivity measured with a g-counter (Perkin-Elmer 2470 Wizard). The percentage of injected dose per gram of tissue (%ID/g) was calculated. Mean and standard deviation (mean ± SD) were determined.

2.8. Ethics statement

All procedures had previously been reviewed by the responsible regional Ethics Committee, and were carried out in strict accordance with the UKCCCR guidelines [26].

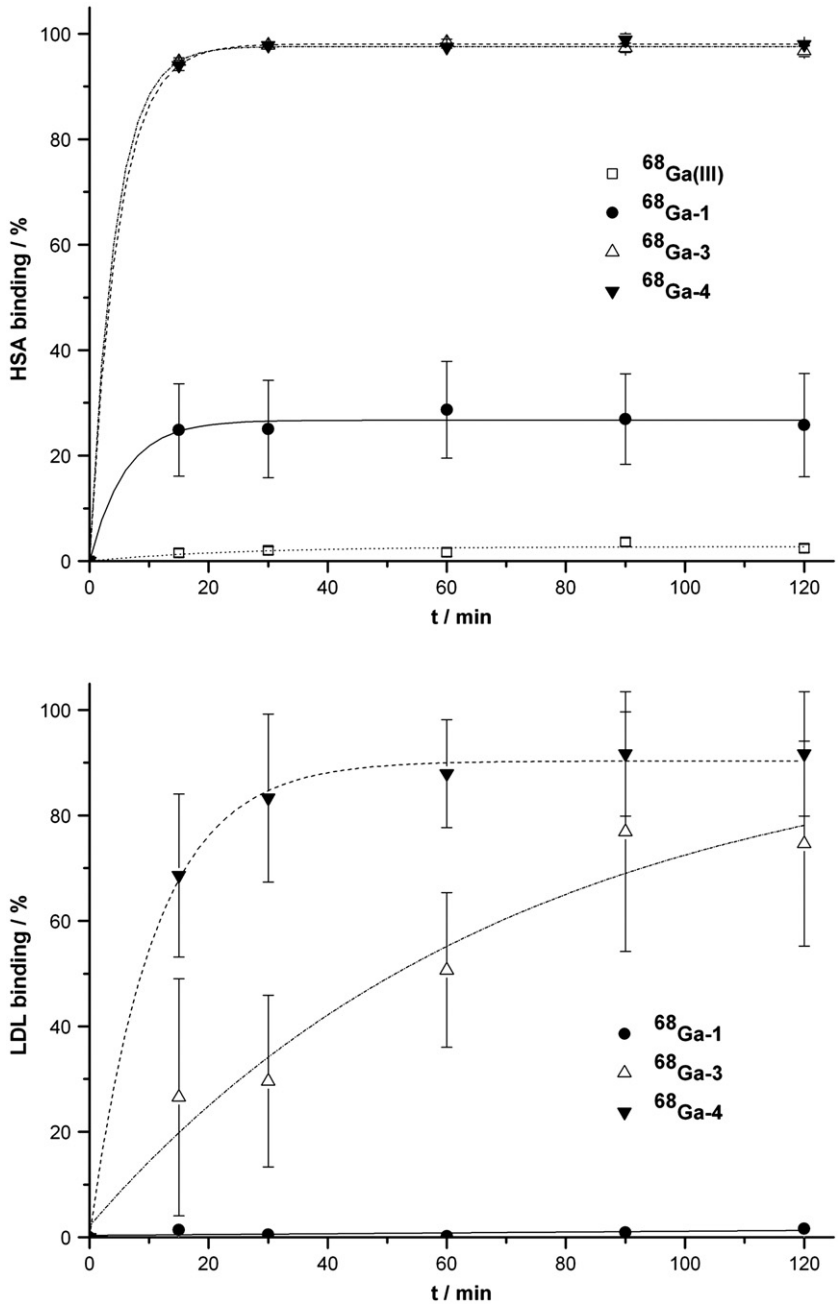

Fig. 7. Binding of the ^{68}Ga-labelled tetrapyrrole derivatives to human serum albumin and low-density lipoprotein. Compounds were incubated in a buffered plasma protein solution at 37 °C. The amounts of the compound plasma protein bonded were determined by size exclusion HPLC.

3. Results and discussion

3.1. Radiochemistry

Initial labelling experiments of the water-soluble compounds **1** and **2** using the post-processed aqueous generator eluate and conventional heating (oil bath at 90 °C) produced only a low labelling. Only 3 ± 1% and 19 ± 5% were achieved for [^{68}Ga]-**1** and [^{68}Ga]-**2**, respectively, within 15 min of heating (Fig. 1). Thus, a modified labelling protocol was required for a more efficient labelling.

Microwave irradiation facilitates a high-energy influx into chemical reactions. According to the Arrhenius equation, a higher energy transfer to the reactants generally results in shorter reaction times and increased chemical yield. Hence, this powerful tool is also highly practical in radiochemistry, especially when short-lived radionuclides are used [27].

Using a microwave-enhanced approach, labelling yields of 69 ± 3% for [^{68}Ga]-**1** after 5 min and 49 ± 9% for [^{68}Ga]-**2** after 7 min were obtained. Extended reaction times resulted in a deceased labelling yield which is most likely being caused by decomposition of the compound. The time dependency of labelling yields was significantly improved by a factor of four for [^{68}Ga]-**2** and of about 46 for [^{68}Ga]-**1** using the same concentration of labelling precursor in the labelling mixture (Fig. 1). In these cases, the use of microwave irradiation leads to a significant improvement in labelling yields.

In contrast, ^{68}Ga-labelling of the lipophilic porphyrin derivatives **3**, **4** and **5** was achieved using n.c.a. ^{68}Ga(acac)$_3$ as the labelling agent. ^{68}Ga(acac)$_3$ was obtained from the generator eluate using a modified post-processing protocol. Microwave assisted radiosynthesis under anhydrous conditions was conducted as published previously [25]. This approach resulted in a rapid labelling reaction with a labelling of 82 ± 6% for [^{68}Ga]-**3**. In parallel, a labelling of 83 ± 6% was obtained for [^{68}Ga]-**4** within only 5 min (Fig. 2). The lipophilic porphyrin derivative **5** was labelled in a labelling yield of 42 ± 7% within 7 min.

Purification of the labelled porphyrins and chlorins was readily achieved by solid-phase extraction on an anion exchange resin. Non-chelated amounts of ^{68}Ga-activity were retained on the cartridge when the labelled product was eluted with phosphate-buffered saline. In this manner, [^{68}Ga]-**1**, [^{68}Ga]-**3** and [^{68}Ga]-**4** were formed at a radiochemical purity of >95%, ready for intravenous administration (Fig. 3). Conversely, the derivatives [^{68}Ga]-**2** and [^{68}Ga]-**5** could not be purified in a sufficient quality for *in vitro* or *in vivo* applications. Summarized results for the radiolabelling and purification of the porphyrin derivatives are listed in Table 1. The structures of the ^{68}Ga-labelled tetrapyrrole derivatives are shown in Fig. 4.

Since gallium-68 is predominantly used for indirect radiolabelling of targeting vectors via conjugation to macrocylcic chelators such as DOTA or NOTA [4], the reported labelling approach represents a direct ^{68}Ga-complexation of the targeting molecule by itself. By adaptation the analogy of ^{68}Ga^{III} to Fe^{III} metal complex chemistry of the tetrapyrrol system, five different porphyrin derivatives could be labelled with generator-derived gallium-68. This achievement is a new exploration of a direct ^{68}Ga-labelling of natural products potentially suitable for PET.

3.2. In vitro complex stability

To examine the ^{68}Ga-porphyrin complex stability, transmetallation and transchelation experiments were conducted with [^{68}Ga]-**1**, [^{68}Ga]-**3** and [^{68}Ga]-**4**. Transchelation of ^{68}Ga to DTPA (Table 2) or to *apo*-transferrin (Fig. 5) was not observed over a period of two hours. Moreover, a high complex stability in terms of displacement of the ^{68}Ga^{III} core via transmetallation reactions was observed in the presence of Fe^{III} ions (Table 2).

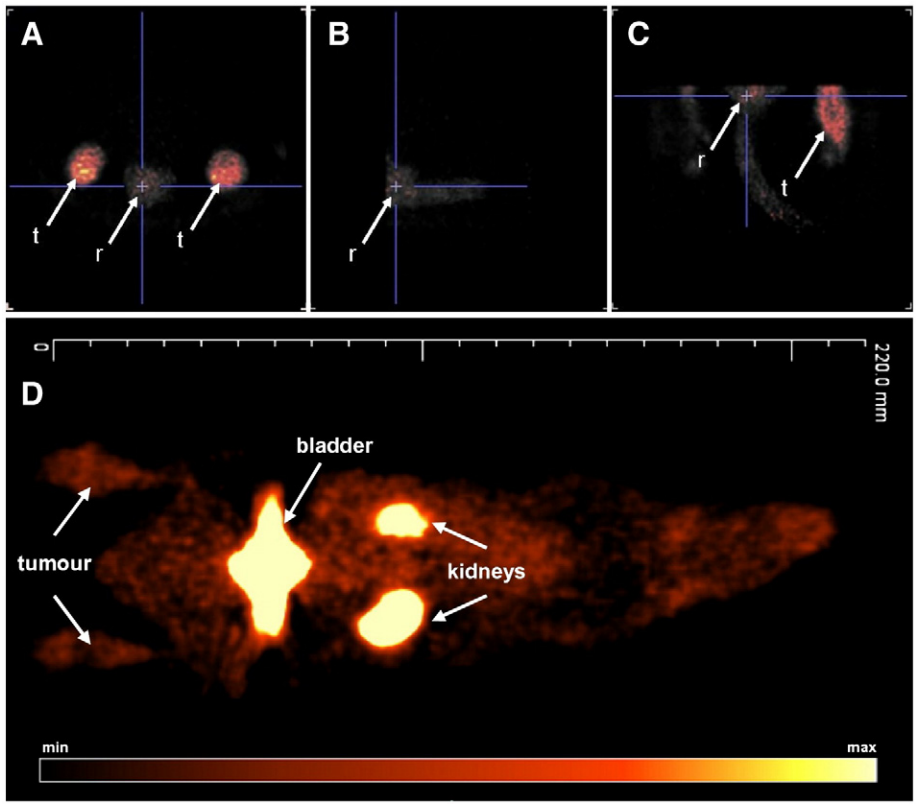

Fig. 8. PET/PET co-registration (10 min p.i) of the hind legs and testes after the injection of [^{68}Ga]-**1** (top). (A) Coronal, (B) sagittal and (C) transversal view. (t) denotes the tumour lesions, (r) denotes the reference region. Dynamic PET data were collected over 60 min. Representative static whole body PET image were obtained 60–80 min after tracer administration (D). Rats were injected with 19 MBq [^{68}Ga]-**1** (5-15 nmol), anesthetized with sodium pentobarbital (40 mg/kg).

No substantial release of ^{68}Ga from the lipophilic chelates [^{68}Ga]-**3** and [^{68}Ga]-**4** was observed in blood serum over a period of two hours. In contrast, a half-life of only 72 min in human serum was determined for the hydrophilic compound [^{68}Ga]-**1**. This however has to be attributed to rapid metabolism of the native porphyrin in blood and is probably unrelated to actual transchelation. Thus, the tested compounds possessed a sufficient complex stability for further investigation in *in vitro* or *in vivo* applications (Fig. 6).

3.3. Plasma protein binding

Uptake of the ^{68}Ga-labelled tetrapyrroles into LDL and HSA was determined using size-exclusion chromatography (Fig 6). As expected, comparison of radioactive and UV detection revealed the same retention time for the formed ^{68}Ga-labelled proteins and the pure protein sample. These findings indicate that both proteins, HSA and LDL, remain unchanged upon interaction with the ^{68}Ga-labelled tracer. For this reason it is to be expected that HSA and LDL may serve as vehicles for the ^{68}Ga-labelled tracers, thereby mediating radioactivity uptake into tumour lesions and inflammatory tissue. An HSA binding of up to 97% of the applied dose and a LDL uptake of more than 75% over a period of 120 min was found for the lipophilic porphyrin complexes [^{68}Ga]-**3** and [^{68}Ga]-**4** (Fig. 7). In contrast, the more polar compound [^{68}Ga]-**1** showed a HSA binding of only 26 ± 9% and an insignificant LDL binding.

Contrary to our earlier report [25], this study was devoted to *in vitro* characterisation of a variety of ^{68}Ga-labelled tetrapyrroles. So far, the mechanism of tumour uptake of intact porphyrins and chlorins is only poorly understood and most attempts to increase tumour uptake have thus far focused on increasing the lipid-solubility. Both plasma protein and lipoprotein mediated endocytosis and an enhanced permeation and retention effect have been discussed as accumulation mechanism [17–20]. Our study confirmed that the ^{68}Ga labelled metalloporphyrins still show a pronounced uptake into the LDL-vehicle, implying that further investigation of this class of compounds is warranted. Thus, these finding combined with our radiochemical procedures might spark interest in ^{68}Ga-tetrapyrrole PET.

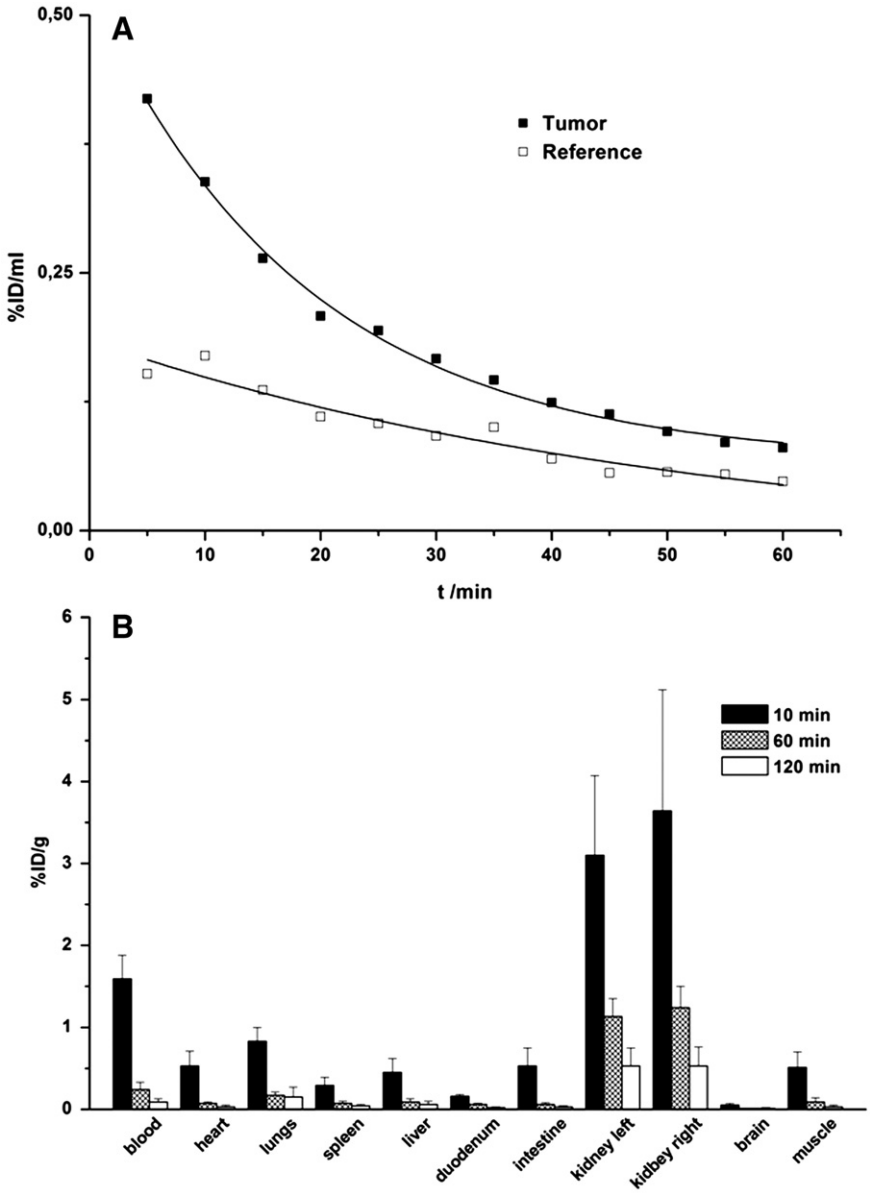

Fig. 9. Pharmacokinetic profile of the radiolabeled tetrapyrrole [^{68}Ga]-1. PET time-activity-curve (A) for the tumour lesions (diamonds) and the reference region (squares) were generated form reconstructed PET data 0-60 min after tracer injection. Ex vivo biodistribution studies were evaluated in health rats (B). Mean and standard deviation (mean ± SD, n = 3) were determined.

3.4. MicroPET imaging and biodistribution studies

A preliminary micro-PET study was conducted in a Sprague-Dawley rat bearing a DS sarcoma on each hind foot dorsum. The reconstructed PET images suggest increased uptake of the injected [^{68}Ga]-**1** in both tumour lesions (Fig. 8A,B,C). Whole body PET data were obtained from the same animal scanned 60-80 min post tracer administration. This PET image clearly visualised the hind legs bearing the tumour lesions as compared to the front legs, where no tumour tissue was inoculated (Fig. 8D). Renal clearance of the labelled compound was indicated by highly focal radioactivity concentration in the kidneys and the bladder. To determine the *in vivo* pharmacokinetic profile of [^{68}Ga]-**1**, the time-activity-curve were reconstructed from the 60-min dynamic PET scan (Fig. 9A). A maximum tumour uptake of about 0.5% of the injected dose per cm^3 (%ID/ml) was reached 7 min after injection. The concentration of radioactivity in the tumour tissue equilibrates after 10 min. However, the uptake and washout rate of the radiotracer is significantly slower for the tumour tissue than for the reference region in the testes. Compared to the reference region, a stable tumour to tissue ratio of 2 ± 0.3 is achieved. In addition, the whole body biodistribution of [^{68}Ga]-**1** was investigated in healthy rats. As already indicated by PET imaging, a rapid clearance of the tracer from the blood pool and non-targeted tissue via the kidneys was observed. No specific accumulation in the organs was detected (Fig. 9B).

For comparison, tumour tissue accumulation studies with gallium metalloporphyrins in hamsters demonstrated comparable ratios 24 hours after compound administration [18]. The obtained distribution is furthermore different from the pharmacokinetic profile obtained for 'free' $^{68}Ga^{III}$ [28]. While a fast blood pool clearance as essential parameter for contrast imaging could be clearly demonstrated, an optimization of the accumulation and retention of the radiotracer in the tumour lesion has to be achieved.

Motivated by this preliminary feasibility study, more detailed investigations and validations of radiolabeled tetrapyrroles are therefore warranted to verify their potential as PET imaging agent for tumour and inflammation *in vivo*. For this purpose, a set of both water-soluble and lipophilic porphyrin derivatives that was successfully radiolabelled are hereby available for further studies.

4. Conclusion

Five porphyrin derivatives were labelled with ^{68}Ga in a microwave-enhanced radiosynthesis, both under aqueous and anhydrous conditions. This radiosynthesis technique provided rapid ^{68}Ga incorporation in high RCY using nanomolar concentrations of tetrapyrrole precursor. Evidently, the use of n.c.a. [^{68}Ga]Ga acetylacetonate as the labelling agent allows the formation of ^{68}Ga-labelled complexes from lipophilic, water-insoluble chelators. Purification and formulation of the labelled products for biological evaluation were readily achieved by solid-phase extraction. *In vitro* evaluation illustrates kinetic inertness and high thermodynamic stability over a period of 2 h. Moreover, as basic requirement for *in vivo* application, the labelled products remained intact in human serum over the same period of time. In a proof of concept PET study, the ^{68}Ga-labelled tetrapyrrole complexes suggest the suitability of these novel tracer candidates for PET imaging. However, these compounds are yet to be subjected to detailed validation studies to determine the exact nature of uptake in the target region. Thus, the reported achievements will contribute to further developments of ^{68}Ga-labelled porphyrins as molecular imaging probe.

Acknowledgments

The authors are grateful to M. Jahn and H. Schieferstein for technical support and to C. Burchardt for helpful discussions. We gratefully acknowledge the "Fonds der chemischen Industrie" for support.

References

[1] Bhat MR. Nuclear data sheets for A = 68. Nuclear Data Sheets 1988;55:1–70.
[2] Roesch F, Riss PJ. The renaissance of the Ge/Ga radionuclide generator initiates new developments in Ga radiopharmaceutical chemistry. Curr Top Med Chem 2010;10:1633-68.
[3] Brechbiel MW. Bifunctional chelates for metal nuclides. Q J Nucl Med Mol Imaging 2008;52:166-73.
[4] Weiner R, Thakur M. Chemistry of gallium and indium radiopharmaceuticals. In: Welch M, Redvanly C, editors. Handbook of Radiopharmaceuticals: Radiochemistry and Applications. Chichester: Wiley; 2003. p. 363-400.
[5] Falk J. Porphyrins and metalloporphyrins. New York: Elsevier; 1975.
[6] Buchler J, Eikelmann G, Puppe L, Rohbock K, Schneehage H, Weck D. Metallkomplexe mit Tetrapyrrol-Liganden. III. Darstellung von Metallkomplexen des Octaäthylporphins aus Metallacetylacetonaten. Liebigs Ann Chem 1971;745: 135-51.
[7] Fleischer E. Structure of porphyrins and metalloporphyrins. Accounts Chem Res 1970;3:105-12.
[8] Juzeniene A, Peng Q, Moan J. Milestones in the development of photodynamic therapy and fluorescence diagnosis. Photochem Photobiol Sci 2007;6:1234-45.
[9] Hamblin MR, Newman EL. On the mechanism of the tumour-localising effect in photodynamic therapy. J Photochem Photobiol B 1994;23:3-8.
[10] Ochsner M. Photophysical and photobiological processes in the photodynamic therapy of tumours. J Photochem Photobiol B 1997;39:1–18.
[11] Pandey SK, Gryshuk AL, Sajjad M, Zheng X, Chen Y, Abouzeid MM, et al. Multimodality agents for tumor imaging (PET, fluorescence) and photodynamic therapy. A possible "see and treat" approach. J Med Chem 2005;48:6286-95.
[12] Jia ZY, Deng HF, Pu MF, Luo SZ. Rhenium-188 labelled meso-tetrakis[3,4-bis(carboxymethyleneoxy)phenyl] porphyrin for targeted radiotherapy: preliminary biological evaluation in mice. Eur J Nucl Med Mol Imaging 2008;35:734-42.
[13] Sarma HD, Das T, Banerjee S, Venkatesh M, Vidyasagar PB, Mishra KP. Biologic evaluation of a novel 188Re-labeled porphyrin in mice tumor model. Cancer Biother Radiopharm 2010;25:47-54.
[14] Easson MW, Fronczek FR, Jensen TJ, Vicente MG. Synthesis and in vitro properties of trimethylamine- and phosphonate-substituted carboranylporphyrins for application in BNCT. Bioorg Med Chem 2008;16:3191-208.
[15] Kralova J, Kejik Z, Briza T, Pouckova P, Kral A, Martasek P, et al. Porphyrin-cyclodextrin conjugates as a nanosystem for versatile drug delivery and multimodal cancer therapy. J Med Chem 2009;53:128-38.
[16] Yumita N, Han QS, Kitazumi I, Umemura S. Sonodynamically-induced apoptosis, necrosis, and active oxygen generation by mono-l-aspartyl chlorin e6. Cancer Sci 2008;99:166-72.
[17] Nakajima S, Takemura T, Sakata I. Tumor-localizing activity of porphyrin and its affinity to LDL, transferrin. Cancer Lett 1995;92:113-8.
[18] Nakajima S, Hayashi H, Omote Y, Yamazaki Y, Hirata S, Maeda T, et al. The tumour-localizing properties of porphyrin derivatives. J Photochem Photobiol B 1990;7: 189-98.
[19] Firnau G, Maass D, Wilson B, Jeeves W. 64Cu-labelling of hematoporphyrin derivative for non-invasive measurements of tumor uptake. In: Doiron D, Gomer C, editors. Porphyrin localization and treatment of tumors. New York: Liss; 1984. p. 115-32.
[20] Fawwaz RA, Winchell HS, Frye F, Hemphill W, Lawrence JH. Localization of 58Co and 65Zn-hematoporphyrin complexes in canine lymph nodes. J Nucl Med 1969;10:581-5.
[21] Mahhood A, Jones A. Technetium radiopharmaceuticals. In: Welch M, Redvanly C, editors. Handbook of Radiopharmaceuticals: Radiochemistry and Applications. Chichester: Wiley; 2003. p. 323-62.
[22] Montforts M, Meier A, Haake G, Höper F. A taylor made lipophilic chlorin for photodynamic tumor therapy. Tetrahedron Lett 1991;32:3481-2.
[23] Haake G, Meier A, Montforts F-P, Scheurich G, Zimmermann G. Synthese von Chlorinen aus dem roten Blutfarbstoff Hämin. Liebigs Annalen der Chemie 1992;1992:325-36.
[24] Zhernosekov KP, Filosofov DV, Baum RP, Aschoff P, Bihl H, Razbash AA, et al. Processing of generator-produced 68Ga for medical application. J Nucl Med 2007;48:1741-8.
[25] Zoller F, Riss PJ, Montforts FP, Rosch F. Efficient post-processing of aqueous generator eluates facilitates Ga-68-labelling under anhydrous conditions. Radiochimica Acta 2010;98:157-60.
[26] Workman P, Twentyman P, Balkwill F, Balmain A, Chaplin D, Double J, et al. United Kingdom Co-ordinating Committee on Cancer Research (UKCCCR) Guidelines for the Welfare of Animals in Experimental Neoplasia (Second Edition). Br J Cancer 1998;77:1–10.
[27] Elander N, Jones JR, Lu S-Y, Stone-Elander S. Microwave-enhanced radiochemistry. Chem Soc Rev 2000;29:239-49.
[28] Mitreĭkin VF, Fadeev NP, Savel'eva OP. Study of gallium-67 citrate distribution in rat tumors. Vopr Onkol 1976;22:77-81.